Electronic Supplementary Information
Experimental Demonstrations of Spontaneous, Solar-Driven Photoelectrochemical Water Splitting

Joel W. Ager,*[ab] Matthew Shaner,[cd] Karl A. Walczak,[ab] Ian D. Sharp,[ae] and Shane Ardo[f]

[a]Joint Center for Artificial Photosynthesis, Lawrence Berkeley National Laboratory, Berkeley, CA, USA E-mail: JWAger@lbl.gov

[b]Materials Sciences Division, Lawrence Berkeley National Laboratory, Berkeley CA, USA

[c]Joint Center for Artificial Photosynthesis, California Institute of Technology, Pasadena, CA, USA

[d]Division of Chemistry and Chemical Engineering, California Institute of Technology, Pasadena, CA, USA

[e]Physical Biosciences Division, Lawrence Berkeley National Laboratory, Berkeley CA, USA

[f]Department of Chemistry, and Department of Chemical Engineering and Materials Science, University of California Irvine, Irvine, CA, USA

The solar-to-hydrogen (STH) conversion efficiency and operation stability of 47 reports of spontaneous, solar-driven water splitting are compiled in Tables 2 – 5 of the main text. Additional analysis on the electrolyte conditions employed and the reported STH conversion efficiency and device longevity are reported here.

Figure S1 shows a pie chart of these 47 reports binned by the pH of the electrolyte into three pH ranges: acidic, 0-4; near-neutral; 4-10; and basic, 10-14. There are an approximately equal number of acidic and basic demonstrations; about a quarter of the demonstrations used near-neutral pH conditions.

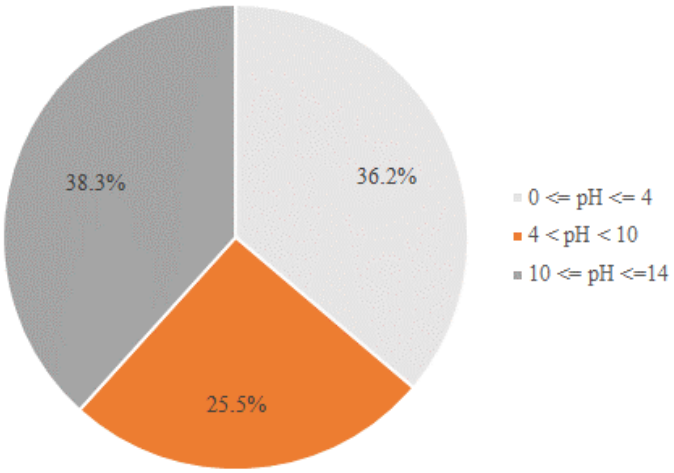

Figure S1. Pie chart showing the relative proportion of devices operating within a specified pH regime.

Figure S2 provides further analysis of the data shown in Figure S1 by separating each pH range by type of system, including the number of junctions:

- 2J, SLJ, 2 junction tandem PV with at least one semiconductor–liquid junction (SLJ), cf. Table 2;
- 2J, isolated PV, 2J tandem PV with all PV junctions "buried" including PV + electrolyzer approaches, cf. Table 3
- 3J, SLJ, 3 junction tandem PV with at least one semiconductor–liquid junction (SLJ), cf. Table 4;
- and 3J, isolated PV, 3J tandem PV with all PV junctions "buried" including PV + electrolyzer approaches, cf. Table 5.

Nearly every device category has a demonstration in one of the previously defined pH ranges.

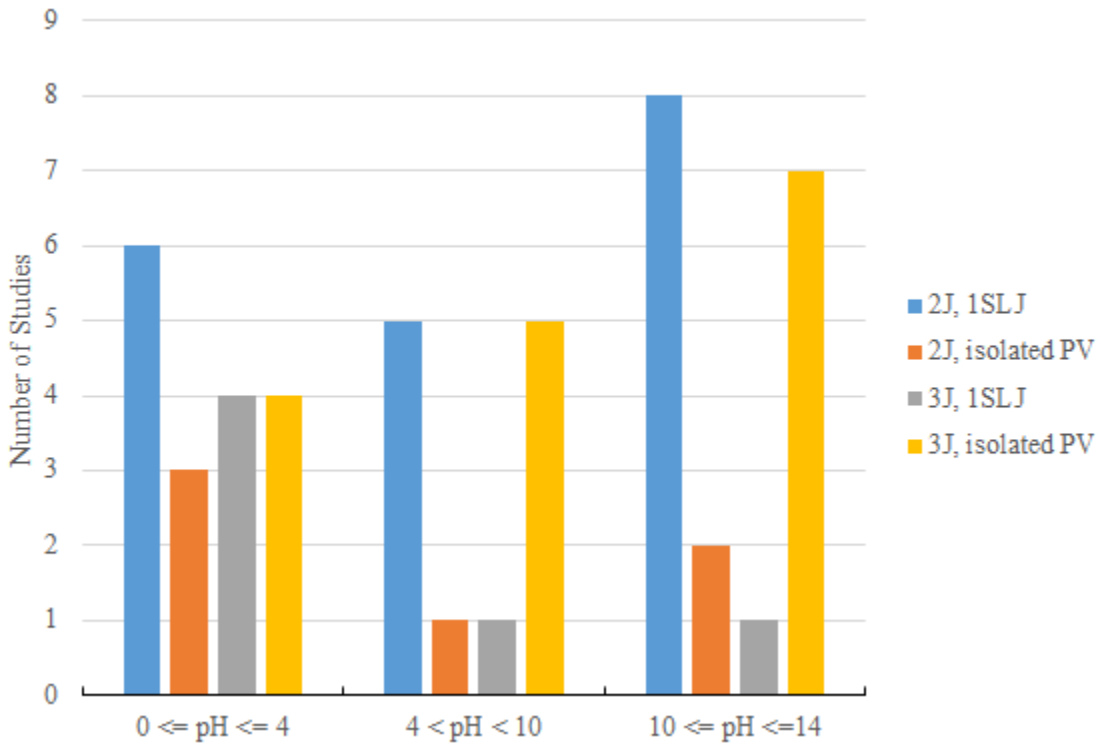

Figure S2. Histogram of the number of reports for each electrolyte pH range, organized by device configuration.

Figure S3 graphs the STH conversion efficiency versus pH of the electrolyte, employing the same device configurations as in Figure S2. This illustrates that even the largest reported STH conversion efficiencies (i.e. those close to or exceeding 10%) were operated over a wide range of pH values, from 0 to 14. The only device configuration that does not have a reported STH efficiency greater than 10% is the 3J, SLJ category.

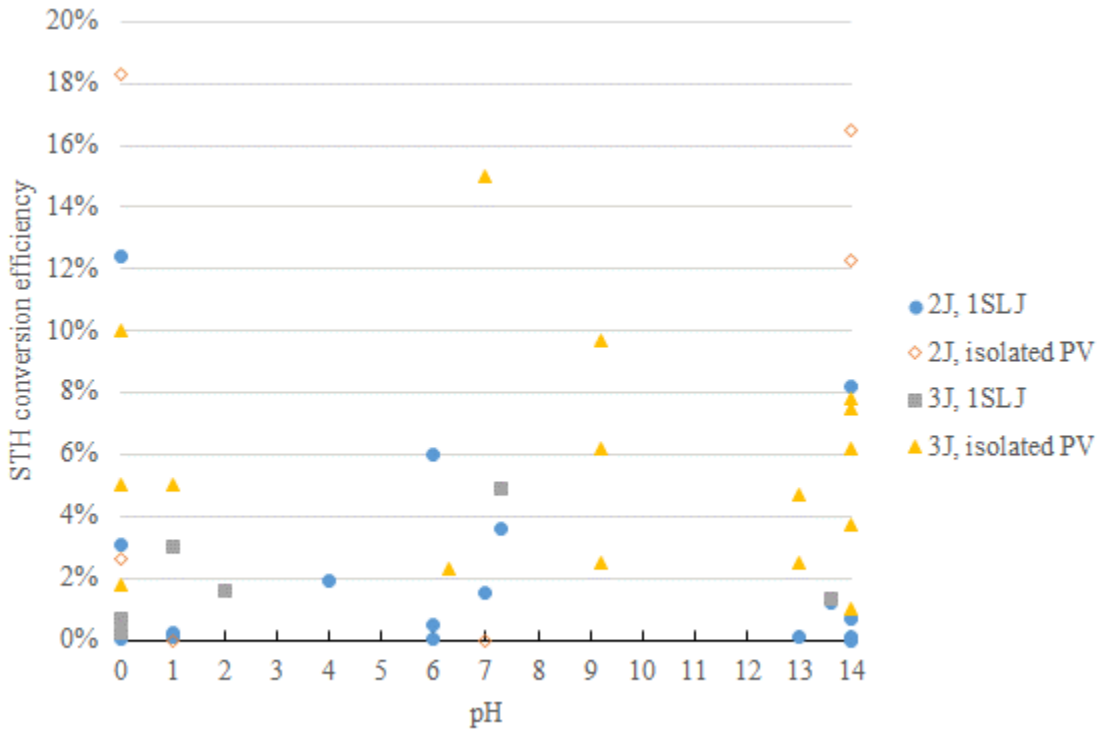

Fig. S3. Reported solar-to-hydrogen (STH) conversion efficiency versus pH. See bulleted list in text for explanation of the legend.

Figures S4 and S5 analyze reported longevity. Figure S4 shows the reported longevity sorted by device type. The devices with isolated PV elements tend to have longer reported lifetimes, but there are very few demonstrations exceeding one week in duration. Figure 5 graphs reported longevity versus the pH of the electrolyte. Again, there are very few reports of long-term device operation at any electrolyte pH. Three studies have reported a lifetime over 100 hr. Two of those used a 3J with isolated PV elements and the other employed 3 PV junctions with one being an SLJ.

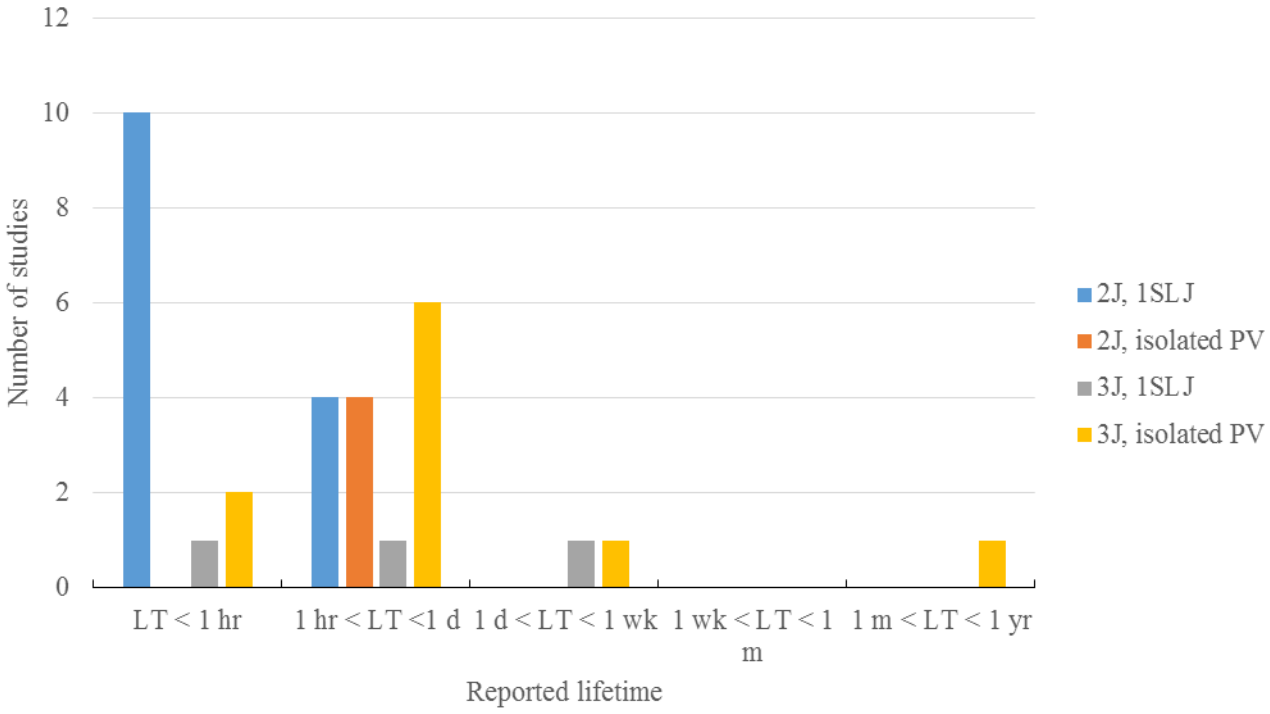

Figure S4. Histogram of the number of reports for each lifetime range, organized by device configuration. The studies that did not report a lifetime were not included in the figure above.

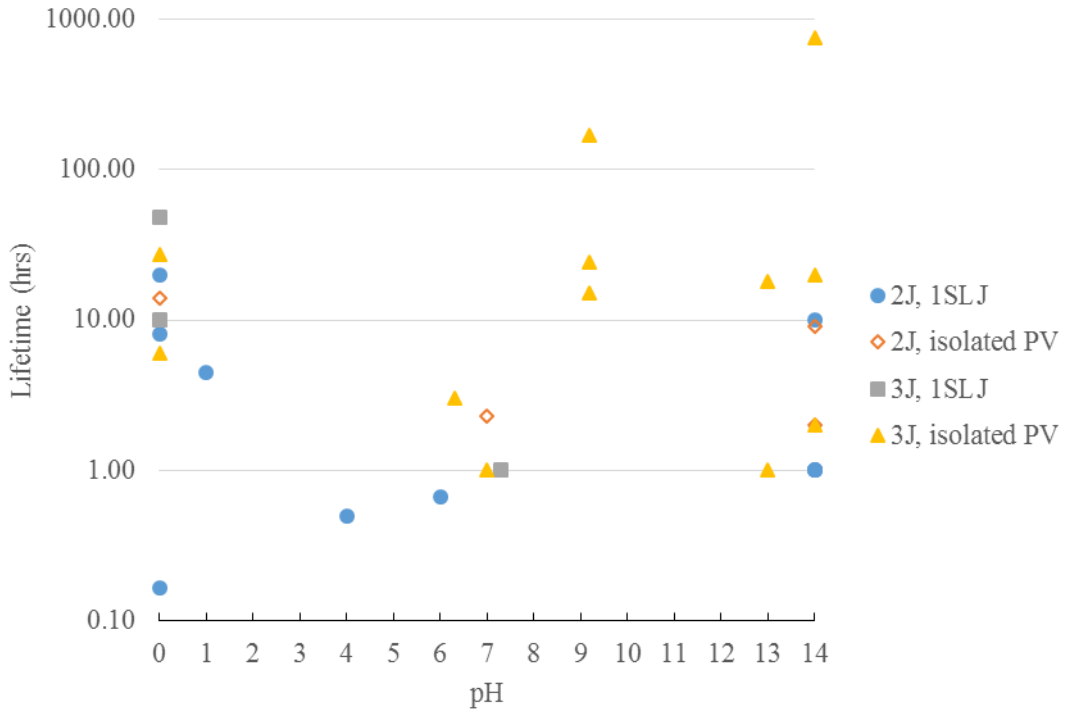

Figure S5. Reported lifetime in hours graphed versus pH. See bulleted list in text for explanation of the legend.